LMSEAT-33892

Pre-Test Analysis for the Alpha Magnetic Spectrometer (AMS-02) Magnet Support Strap Assembly Dynamic Test

Prepared by

Lockheed Martin Space Operations
Houston, TX

For

National Aeronautics and Space Administration
Lyndon B. Johnson Space Center

March 5, 2002

Pre-Test Analysis for the AMS-02 Strap Dynamic Test

Prepared by:

Original signed by Chris Tutt
Chris Tutt
Dynamics Analyst
Loads and Dynamics Analysis Section, LMSO

Reviewed by:

Original signed by Carl Lauritzen
Carl Lauritzen
Dynamics Analyst
Loads and Dynamics Analysis Section, LMSO

Approval:

Original signed by Elonsio Rayos
Elonsio Rayos
Manager, Loads and Dynamics Analysis Section
Mechanical Systems Analysis Department, LMSO

Original signed by Trent Martin
Trent Martin
Structural Analysis Lead, AMS-02
Project Integration Office, LMSO

Original signed by Kenneth J. Bollweg
Kenneth Bollweg
Project Manager, AMS-02
Project Integration Office, LMSO

Contents

List of Figures

List of Tables

List of Acronyms

AMS	Alpha Magnetic Spectrometer
FRF	Frequency Response Function
ISS	International Space Station
LMSO	Lockheed Martin Space Operations
SCL	Space Cryomagnetics, Ltd.
SDOF	Single Degree of Freedom
SVP	Structural Verification Plan
VC	Vacuum Case
VLA	Verification Loads Analysis

References

1. JSC 28792B *Alpha Magnetic Spectrometer – 02 Structural Verification Plan for the Space Transportation System and the International Space Station*, December 2001.

2. LMSEAT 33848 *Test Plan for the Dynamic Test of the Magnet Support Strap Assembly for the Alpha Magnetic Spectrometer (AMS)-02*, January 2, 2002 (Proprietary).

3. Fax from John Ross to Trent Martin, re "CTW Ties," October 12, 2001.

4. Nayfeh, Ali and Dean Mook, *Nonlinear Oscillations*, New York: John Wiley and Sons, 1979.

5. E-mail from Trent Martin to Bruce Sommer et al, "Strap Data Received," December 11, 2001.

6. Fax from John Ross to Trent Martin, re "Damping Loss in supports," December 2, 2001

7. Thompson, J. M. T., and H. B. Stewart, *Nonlinear Dynamics and Chaos*, New York: John Wiley and Sons, 1986.

1.0 Introduction

1.1 Background

The Alpha Magnetic Spectrometer-02 (AMS-02) is a 14,000 lb multinational physics experiment designed for launch in the Space Shuttle and deployment on the International Space Station (ISS). The magnetic field for the spectrometer is generated by a large, superconducting electromagnet contained inside the Vacuum Case (VC). A basic picture of the payload is shown in Figure 1.

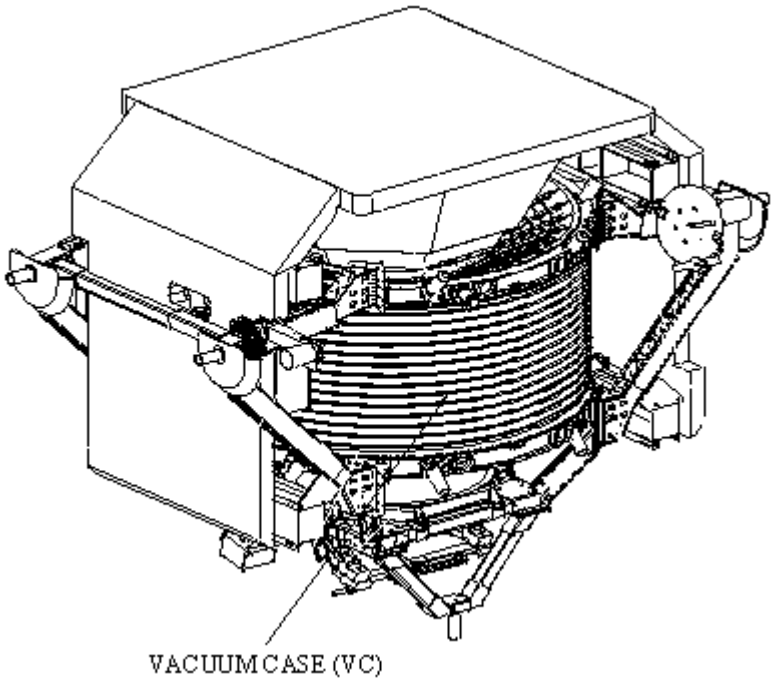

Figure 1: Alpha Magnetic Spectrometer Payload Assembly

The magnet is cooled using superfluid Helium, which is contained in an annular tank that surrounds the magnet itself. Collectively, the magnet/He tank assembly is referred to as the "cold mass." It is attached to the vacuum case by sixteen composite strap systems. This is required to thermally isolate the cold mass from the rest of the AMS.

The cold mass weighs about 4600 lbs. The first few overall modes of the AMS structure consist of the cold mass moving back and forth inside the vacuum case. Because the straps that connect it are nonlinear, the system modes are themselves nonlinear. As described in the AMS-02 Structural Verification Plan (SVP) [1], one of the analytical goals is to develop a linearized model of the structure for use in the Verification Loads Analysis (VLA). Doing that effectively requires a method for accurately predicting nonlinear responses. To that end, the AMS project is planning to conduct an engineering evaluation test of two flight-like straps in a simple configuration to gather frequency response data. Correlation of the results of this test will be a useful first check of the algorithm being proposed.

1.2 Scope

The goal of this document is to describe the development of a nonlinear model of the simplified two-strap system under test. This test is simply a proof-of-concept for the nonlinear modeling techniques. The test configuration is not intended to directly represent the actual AMS structure. The pre-test analysis presented here is strictly confined to simplified one-dimensional test system. Several assumptions were made which are appropriate for this configuration but may not be appropriate for the full AMS payload. These additional complexities will be dealt with in a future report.

The primary model used in development of the pre-test analysis was a closed-form analytical model derived from the nonlinear equation of motion. Verification of this model is the ultimate goal of this test. A nonlinear Nastran model of the test configuration was also developed and data from a series of transient runs provided a preliminary validation of the closed-form solution. Both models will be compared to the measured test data.

2.0 Analysis

2.1 System Under Test

The test configuration is a simple single degree of freedom (SDOF) system consisting of two flight straps set up in a line. Between them is a lumped mass resting on linear bearings that only allow motion in line with the strap axis. This layout is shown in Figure 2 below. Full details of the setup are provided in the dynamic test plan [2].

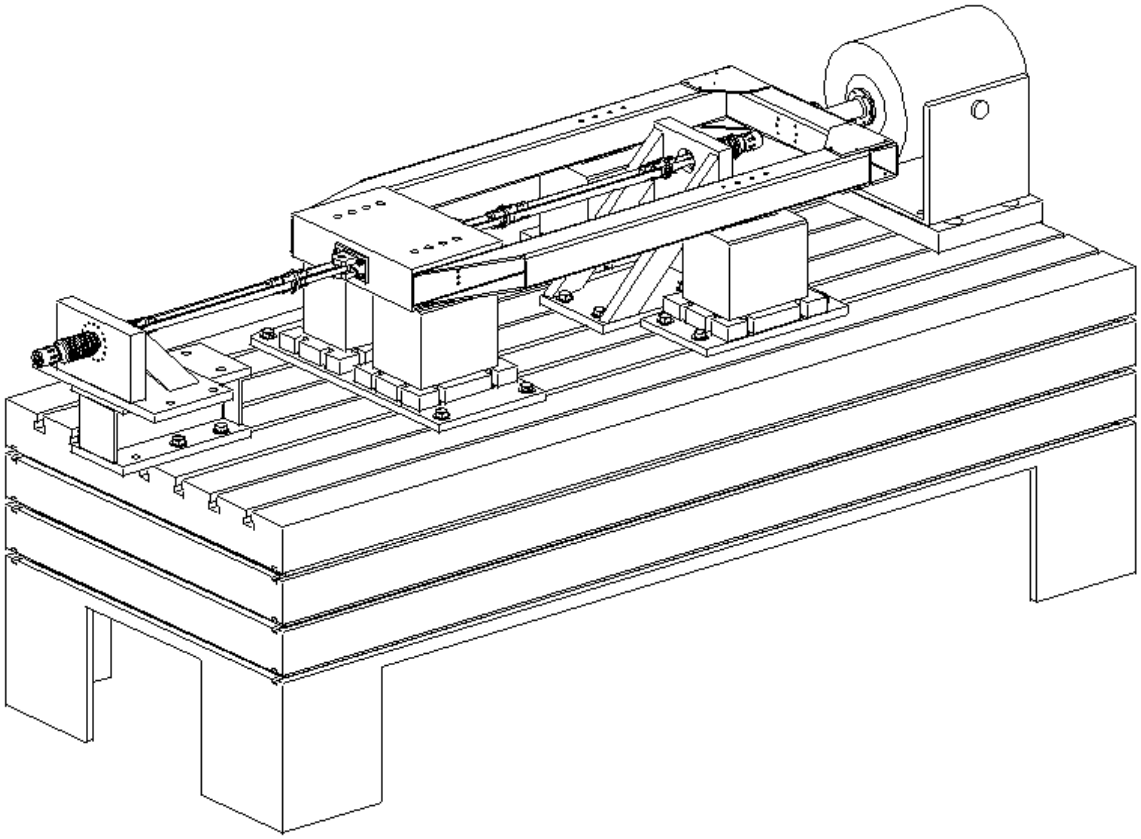

Figure 2: Strap Dynamic Test Layout

There are two separate types of flight straps, designated C1W1 and C2W2. For this test, two C1W1 straps will be used. Stiffness characteristics of the C1W1 straps were provided by the magnet developers [3] and are based on measured test data. This test will not be conducted at cryogenic temperatures, so the "warm" strap stiffness properties were used in this derivation. These properties are summarized in Table 1.

Table 1: C1W1 Warm Stiffness Characteristics

Tensile Load	Deflection from preload point
0	-0.773”
1753 lb	0
1989 lb	0.104”
2157 lb	0.107”
26977 lb	0.360”

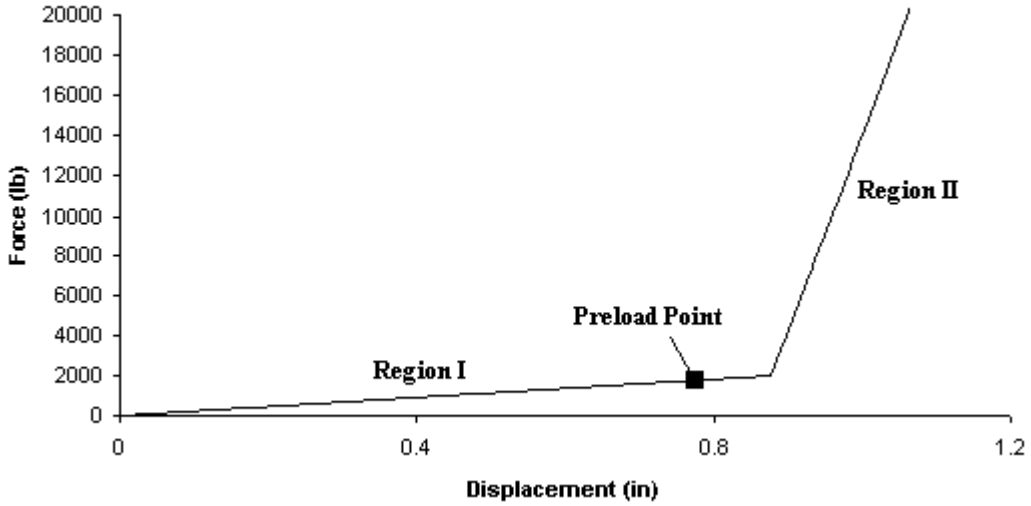

Figure 3: C1W1 Strap Warm Stiffness Curve

Both straps will be preloaded to 1,753 lb, just as they will be for flight. Figure 3 shows two distinct stiffness regions. Below the knee point at 0.104”, the system is extremely soft, with an overall stiffness of 2,269 lb/in. This portion of the curve is referred to as Region I. Above 0.107”, the overall stiffness is 98,258 lb/in and is referred to as Region II. There is a third region between 0.104” and 0.107” where the overall stiffness is 57,487 lb/in. This area was modeled accurately in all calculations, but for the purposes of discussion it will be considered part of Region II.

Figure 4 shows an SDOF representation of the test configuration. Mass m is the mass of the moving test hardware, which includes the central block, the two spacer bars that connect it to the shaker, and the linear bearings. For this test, total moving mass will equal 500 lbs. The strap spring stiffnesses, k^*, match the stiffness curve shown in Figure 3. For convenience, define k_1 as the stiffness in Region I, k_2 as the stiffness in Region II, x_o as the preload point, and x_1 as the displacement at the knee.

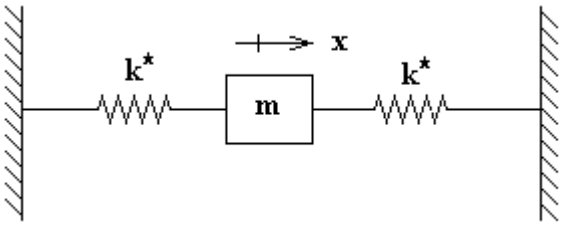

Figure 4: Spring-Mass Representation of Test Configuration

A simple free-body diagram will allow us to derive the overall system stiffness. At $x = x_o$, both straps are at the preload point and both exert an equal and opposite force on the mass of k_1x_o. As x increases towards x_1, the load in the left-hand spring increases to $k_1(x + x_o)$ while the load in the right-hand spring reduces to $k_1(x_o - x)$. The net load on the block is the difference between the two, or $2k_1x$. By similar logic, once $x > x_1$, the net load becomes $(k_1 + k_2)(x - x_1) - k_1x_o$. Using these two formulas, we can build the stiffness relationship for the test system. This is given in Table 2 below.

Table 2: Test Configuration Stiffness Characteristics

Net Load	Deflection from Preload Point
-26039 lb	-0.360”
-646 lb	-0.107”
-472 lb	-0.104”
0 lb	0”
472 lb	0.104”
646 lb	0.107”
26039 lb	0.360”

This stiffness relationship was used to create an SDOF nonlinear Nastran model that was used in the initial validation of the closed form solution.

2.2 Closed-Form Solution

A literature search revealed no closed-form algorithm for predicting steady-state response of a system with bilinear stiffness. It was therefore necessary to develop an approximation to the actual curve that could be solved analytically. The most practical method was to use a least-squares curve fit to find a polynomial that closely matched the bilinear curve. The method of multiple scales, described in Nayfeh and Mook [4], can then be used to derive appropriate frequency response functions.

In addition to being a least-squares fit, some additional restrictions were placed on the polynomial stiffness curve:

- The coefficient of the linear term must equal the Region I stiffness exactly. This makes the solution a perturbation of the Region I linear solution. (Note that this does not mean that the polynomial will match the Region I stiffness exactly. Instead, it means that there will be no α_1 term in the equation below.)

- The polynomial system must have the same equivalent natural frequency at the knee point as the actual system.

- The curve must always increase across the displacement range of interest.

The smallest polynomial that met all these requirements was 11th order:

$$\frac{kx}{m} = \omega_1^2 x + \alpha_3 x^3 + \alpha_5 x^5 + \alpha_7 x^7 + \alpha_9 x^9 + \alpha_{11} x^{11} \qquad (1)$$

where ω_1 = 59.2 rad/s (9.42 Hz), the system natural frequency in Region I, α_3 =-1.06630e6, α_5 = 1.49181e8, α_7 = -3.59564e9, α_9 = 3.31268e10, and α_{11} = -1.05178e11.

The polynomial is displayed in Figure 5 on the next page. A comparison of this curve with the actual one shows a reasonably good match. Although it does begin to break down at higher displacements, these are not expected during this test. In the critical area near the knee point, the polynomial fits quite well.

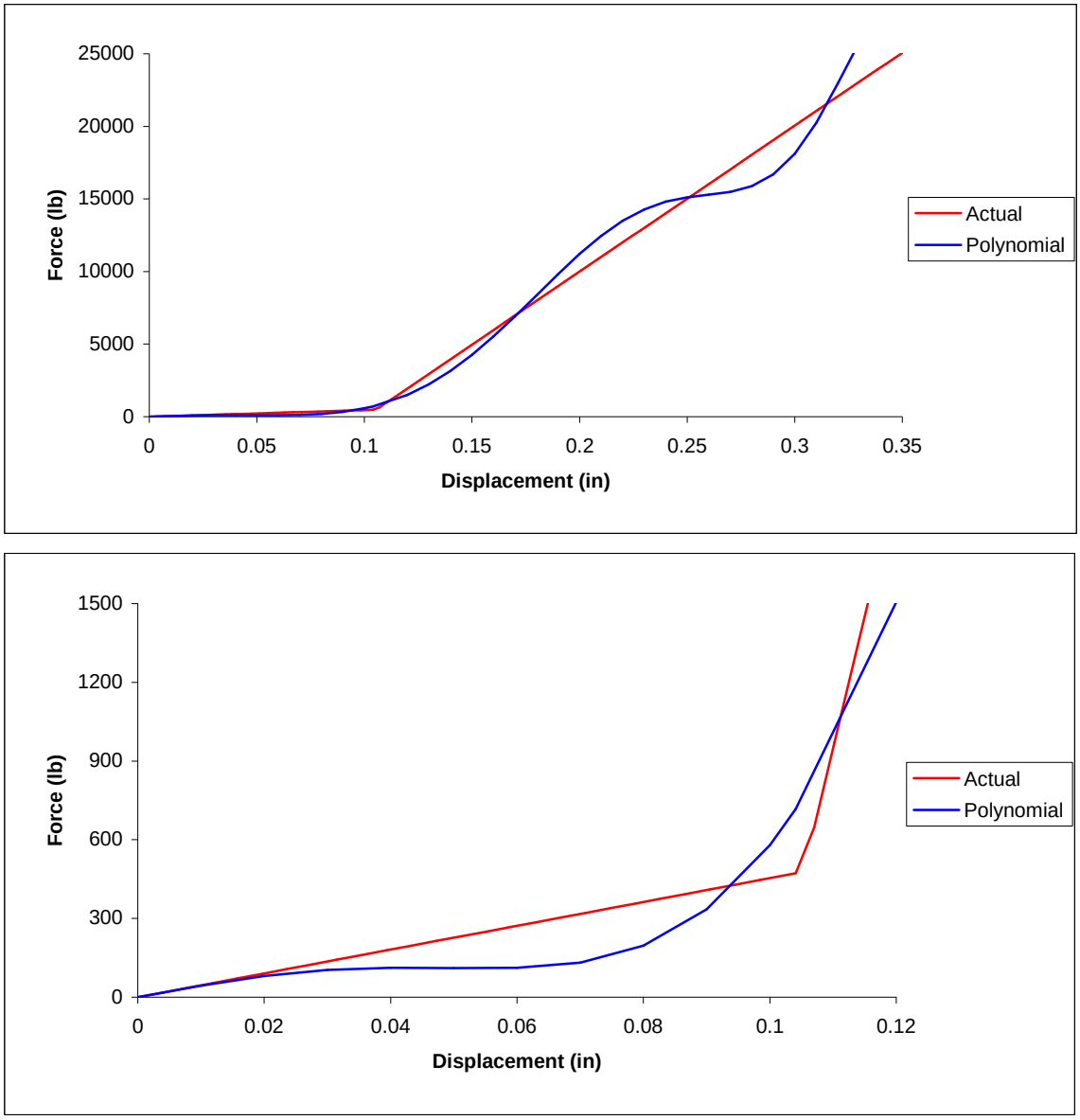

Figure 5: Polynomial Curve Fit Comparison

2.2.1 Frequency Response Functions

Using this stiffness curve, it is possible to derive a frequency response function (FRF) for the nonlinear system. Sample FRFs are shown in Figures 6-8. Unlike linear systems, the function's shape changes with force. In this case, the nonlinearity causes the resonant peak to move rapidly to the right as the load increases. Figure 8 also contains several superharmonic and subharmonic resonant peaks. At the lower force levels of Figures 6 and 7, these responses fall below the knee line and are not relevant.

It is convenient to break the problem up into three segments to be analyzed separately:

- Derivation of the Region I linear solution
- Derivation of the primary nonlinear resonant solution
- Derivation of superharmonic and subharmonic resonant solutions

One valid steady-state vibration solution consists of our system vibrating linearly entirely in Region I. So long as the magnitude does not exceed the knee point at 0.1041", the nonlinearity does not come into play and the system can be analyzed as a standard linear system. This solution is plotted in Figures 6-8 as the blue line. The horizontal purple line designates the knee point.

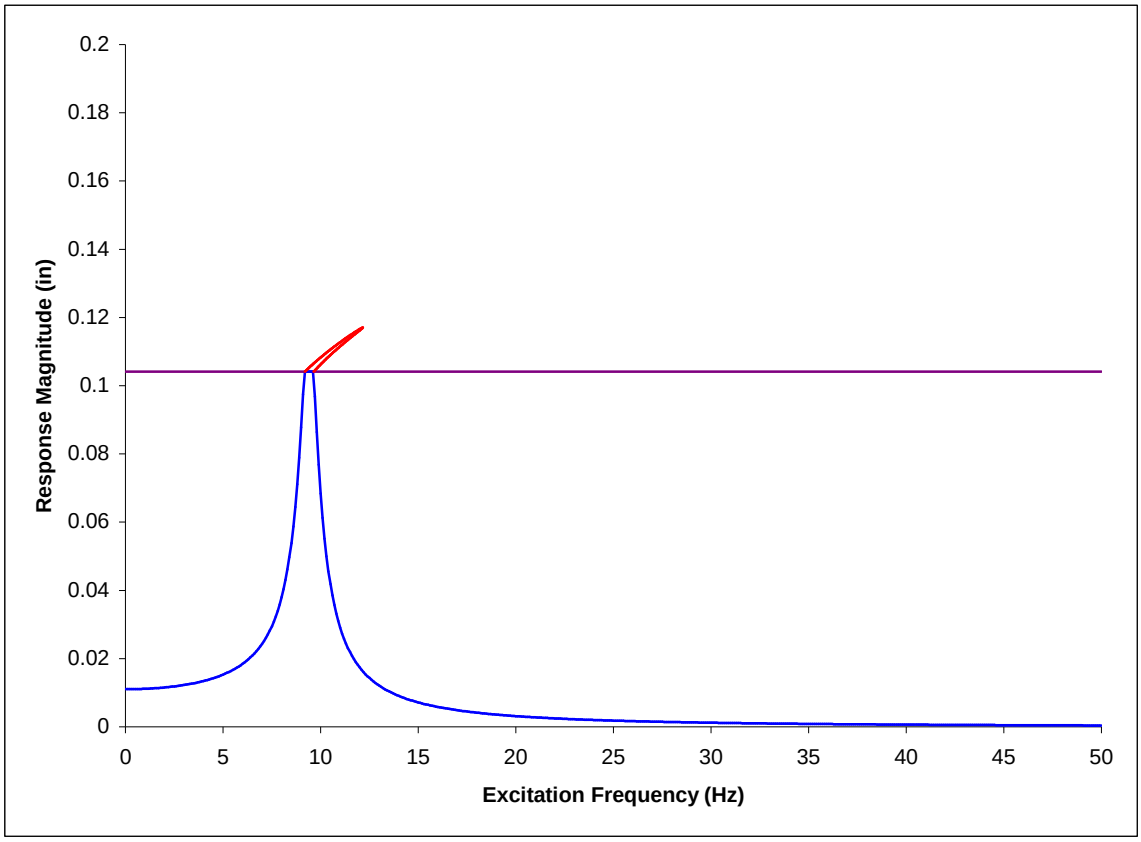

Figure 6: Frequency Response Function for 50 lb Excitation

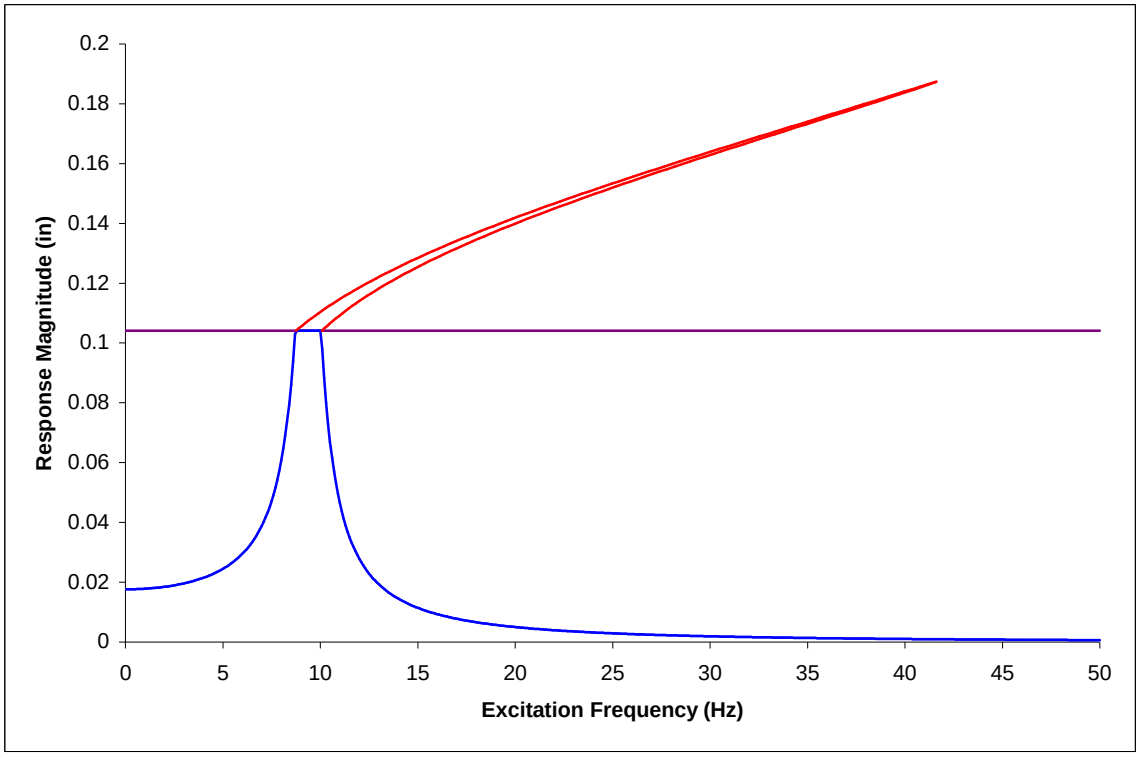

Figure 7: Frequency Response Function for 80 lb Excitation

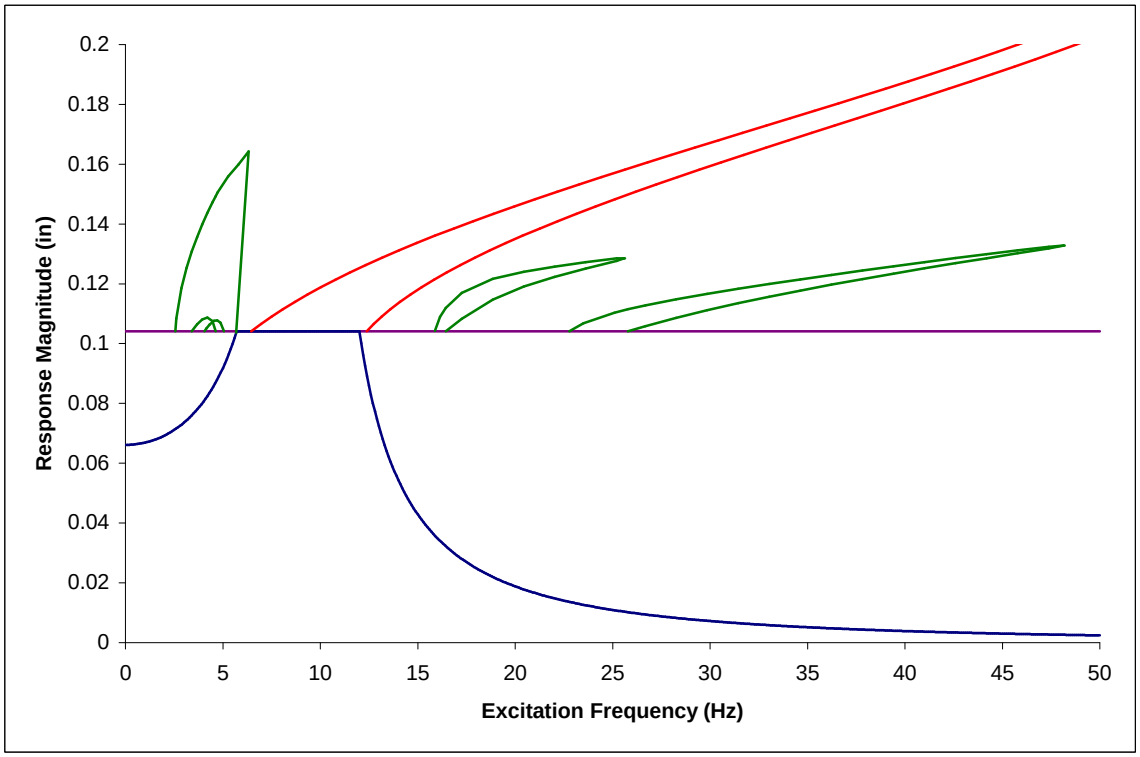

Figure 8: Frequency Response Function for 300 lb Excitation

2.2.2 *Primary Resonance*

The red line in Figures 6-8 corresponds to the nonlinear resonant solution. Where the Region I linear solution only existed below the purple knee line, the resonant solution only exists above it.

To derive this solution, start with the standard equation of motion for an SDOF system:

$$m\ddot{x} + c\dot{x} + k^* x = P\cos\Omega t$$

where k^* in this case refers to the polynomial stiffness defined in Equation 1.

Dividing through by the mass and substituting in the stiffness, we obtain the following:

$$\ddot{x} + 2\varepsilon\mu\dot{x} + \omega_1^2 x + \varepsilon\alpha_3 x^3 + \varepsilon\alpha_5 x^5 + \varepsilon\alpha_7 x^7 + \varepsilon\alpha_9 x^9 + \varepsilon\alpha_{11} x^{11} = \varepsilon p\cos\Omega t \qquad (2)$$

where $\mu \equiv \frac{c}{m}$, $p \equiv \frac{P}{m}$ and ε designates a "small" term. (μ is used instead of the more standard $\zeta\omega_1$ because it will be more convenient later in the derivation.)

Two assumptions have been made in this equation which should be noted. First, damping is assumed to be a single constant for both Region I and Region II. Variable damping, even a different constant for each region, greatly complicates the derivation. It is hoped that an assumption of a single worst-case damping value will lead to conservative predictions. One of the goals of this test will be to check that assumption.

Preliminary damping estimates based on test data for individual straps was provided by Space Cryomagnetics [5,6]. It shows a damping ratio of approximately 1% in Region II and 12% in Region I. Multiplying out the Region II damping ratio gives us a physical damping μ of 2.7872 lb-sec/in. When this damping value is imposed on Region I, it gives a damping ratio of 4.71%. This is significantly less than the actual Region I damping, so using this constant value in the derivation should be conservative.

The second assumption made was that the damping term, the force term, and the nonlinear terms in Equation 2 are small relative to the other terms. Assuming that the first two are small is a very common assumption in dynamics work. Essentially this amounts to assuming that the damped and undamped natural frequencies are identical. For a damping ratio of 4.71%, this would cause an error of 0.11% in frequency, which is trivial.

By assuming the nonlinear terms are small, the nonlinear solution becomes a perturbation off the Region I linear solution. From looking at Figure 5, it is obvious that as the vibration magnitude rises beyond the knee point, this assumption gets worse and worse. For small vibrations close to the knee point, however, it can be expected to give good results. Understanding vibrations around the knee point is the goal of this test, so this assumption should be valid.

With all this in mind, consider Equation 2 above. Assume that x can be represented by two solutions, a primary solution x_o and a perturbation x_1 which is assumed to be small relative to x_o:

$$x \equiv x_o + \varepsilon x_1$$

Also, define the excitation frequency as a function of the Region I natural frequency, ω_1, and a detuning parameter, σ:

$$\Omega \equiv \omega_1 + \varepsilon\sigma$$

The method of multiple scales divides the single time variable in the equation of motion, t, into multiple independent time scales, T_o and T_1, where:

$$T_o = t\,, T_1 = \varepsilon t$$

Both x_o and x_1 are assumed to be functions of T_o and T_1. Substituting these three terms into Equation 2 and dropping all terms of order ε^2 or greater:

$$\frac{\partial^2 x_o}{\partial T_o^2} + 2\varepsilon\frac{\partial^2 x_o}{\partial T_o \partial T_1} + \varepsilon\frac{\partial^2 x_1}{\partial T_o^2} + 2\varepsilon\mu\frac{\partial x_o}{\partial T_o} + \omega_1^2 x_o + \varepsilon\alpha_3 x_o^3 + \varepsilon\alpha_5 x_o^5 + \varepsilon\alpha_7 x_o^7 + \varepsilon\alpha_9 x_o^9 + \varepsilon\alpha_{11} x_o^{11} = \varepsilon p\cos\Omega t \quad (3)$$

Consider all large terms alone:

$$\frac{\partial^2 x_o}{\partial T_o^2} + \omega_1^2 x_o = 0$$

The solution for x_o is thus a standard linear undamped harmonic using Region I properties. All that remains is to find the magnitude of x_o. It is convenient to write it in complex format:

$$x_o = Ae^{i\omega_o T_o} + \overline{A}e^{-i\omega_o T_o}$$

where A is some function of T_1 and $\overline{A}$ denotes its complex conjugate.

Substituting these two terms into Equation 3:

$$\begin{aligned}\frac{\partial^2 x_1}{\partial T_o^2}+\omega_1^2 x_1 = &-2i\omega_1\frac{\partial A}{\partial T_1}e^{i\omega_1 T_o}-2i\mu\omega_1 Ae^{i\omega_1 T_o}-\alpha_3\left(A^3e^{3i\omega_1 T_o}+3A^2\overline{A}e^{i\omega_1 T_o}\right)-\alpha_5\left(A^5e^{5i\omega_1 T_o}\right.\\ &5A^4\overline{A}e^{3i\omega_1 T_o}+10A^3\overline{A}^2e^{i\omega_1 T_o}\left.\right)-\alpha_7\left(A^7e^{7i\omega_1 T_o}+7A^6\overline{A}e^{5i\omega_1 T_o}+21A^5\overline{A}^2e^{3i\omega_1 T_o}\right.\\ &+35A^4\overline{A}^3e^{i\omega_1 T_o}\left.\right)-\alpha_9\left(A^9e^{9i\omega_1 T_o}+9A^8\overline{A}e^{7i\omega_1 T_o}+36A^7\overline{A}^2e^{5i\omega_1 T_o}+84A^6\overline{A}^3e^{3i\omega_1 T_o}\right.\\ &+126A^5\overline{A}^4e^{i\omega_1 T_o}\left.\right)-\alpha_{11}\left(A^{11}e^{11i\omega_1 T_o}+11A^{10}\overline{A}e^{9i\omega_1 T_o}+55A^9\overline{A}^2e^{7i\omega_1 T_o}\right.\\ &+165A^8\overline{A}^3e^{5i\omega_1 T_o}+330A^7\overline{A}^4e^{3i\omega_1 T_o}+462A^6\overline{A}^5e^{i\omega_1 T_o}\left.\right)+\frac{p}{2}e^{i\sigma T_1}e^{i\omega_1 T_o}+cc\end{aligned} \tag{4}$$

where *cc* denotes the complex conjugate of all the terms on the right hand side of the equation.

The solution of this differential equation can be shown to be a bounded harmonic solution for all terms of the form $e^{ni\omega_1 T_o}$ with the exception of $n = 1$. In that case, x_1 will contain terms of the form $T_o e^{i\omega_1 T_o}$. These are known as secular terms. They grow without bound as T_o increases. If there is a valid steady-state solution, then secular terms must not exist. Gathering all the secular terms in Equation 4 and setting them equal to zero, we get:

$$\begin{aligned}&2i\omega_1\frac{\partial A}{\partial T_1}+2i\mu\omega_1 A+3\alpha_3A^2\overline{A}+10\alpha_5A^3\overline{A}^2+35\alpha_7A^4\overline{A}^3+126\alpha_9A^5\overline{A}^4\\ &+462\alpha_{11}A^6\overline{A}^5-\frac{p}{2}e^{i\sigma T_1}=0\end{aligned} \tag{5}$$

It now makes sense to write *A* in complex format:

$$A\equiv\frac{a}{2}e^{ib}$$

where *a* and *b* are functions of T_1. The magnitude is divided by 2 so that *a* will equal the magnitude of the harmonic response of x_o. Plugging this into Equation 5:

$$\begin{aligned}&i\omega_1\frac{\partial a}{\partial T_1}-a\omega_1\frac{\partial b}{\partial T_1}+ia\mu\omega_1+\frac{3}{8}\alpha_3a^3+\frac{5}{16}\alpha_5a^5+\frac{35}{128}\alpha_7a^7+\frac{63}{256}\alpha_9a^9\\ &+\frac{231}{1024}\alpha_{11}a^{11}+\frac{p}{2}e^{i(\sigma T_1-b)}=0\end{aligned} \tag{6}$$

For convenience, define a term γ:

$$\gamma\equiv\frac{1}{\omega_1}\left(\frac{3}{8}\alpha_3a^2+\frac{5}{16}\alpha_5a^4+\frac{35}{128}\alpha_7a^6+\frac{63}{256}\alpha_9a^8+\frac{231}{1024}\alpha_{11}a^{10}\right) \tag{7}$$

Equation 6 then becomes:

$$i\omega_1 \frac{\partial a}{\partial T_1} - a\omega_1 \frac{\partial b}{\partial T_1} + ia\omega_1\mu + a\omega_1\gamma - \frac{p}{2}e^{i(\sigma T_1 - b)} = 0$$

To remove the σT_1 term, break this equation into real and imaginary portions:

$$\omega_1 \frac{\partial a}{\partial T_1} + a\omega_1\mu - \frac{p}{2}\sin(\sigma T_1 - b) = 0 \quad (8a)$$

$$-a\omega_1 \frac{\partial b}{\partial T_1} + a\omega_1\gamma - \frac{p}{2}\cos(\sigma T_1 - b) = 0 \quad (8b)$$

By definition, at steady-state conditions the response magnitude *a* must be a constant and the response frequency must be constant and equal to the excitation Ω:

$$\frac{\partial a}{\partial T_1} = 0, \quad \frac{\partial b}{\partial T_1} = \sigma$$

Substituting this into Equations 8a and 8b and combining them:

$$\frac{p^2}{4\omega_1^2 a^2} = \mu^2 + (\sigma - \gamma)^2 \quad (9)$$

Equation 9 is a closed-form relationship between *a* and σ for primary resonance. It is plotted in Figures 6-8 as the red line.

It should be noted that Equation 9 only defines the primary solution, x_o. The perturbation, x_1, has never been explicitly calculated. To calculate x_1, substitute Equation 5 into Equation 4 and solve the resulting differential equation. If this is done, x_1 will be found to be a collection of higher-order harmonics which refine the shape of primary solution. For a first-order approximation, these terms will be ignored.

2.2.3 Superharmonics and Subharmonics

In nonlinear systems, resonances can occur not only when the system is driven at the natural frequency, but also at specific lower frequencies (superharmonic resonances) and higher frequencies (subharmonic resonances). FRFs for these resonances can be calculated using the method of multiple scales, just as they were for the primary resonance. The full derivation will not be repeated again here, but a few differences will be highlighted.

As before, start with the nonlinear equation of motion:

$$\ddot{x} + \omega_1^2 x = -2\varepsilon\mu\dot{x} - \varepsilon\alpha_3 x^3 - \varepsilon\alpha_5 x^5 - \varepsilon\alpha_7 x^7 - \varepsilon\alpha_9 x^9 - \varepsilon\alpha_{11} x^{11} + p\cos\Omega t \qquad (10)$$

One difference between this equation and Equation 2 is the degree of smallness associated with the forcing term, $p\cos\Omega t$. In the derivation of both the primary resonance and these superharmonic and subharmonic resonances, the baseline solution is response of an undamped system with Region I stiffness. When $\Omega = \omega_1$, the undamped equation of motion has no solution. When deriving the primary resonance curve then, the input force must be considered small so that the force term will be introduced to the solution at the same time as the damping term. For Ω away from ω_1, this is not a concern, so it makes more sense to consider the force as a large term.

In the derivation, this means that when you solve the large terms alone for x_o, you get a different baseline solution:

$$x_o = Ae^{i\omega_1 T_0} + \overline{A}e^{-i\omega_1 T_{10}} + \Lambda e^{i\Omega T_o} + \Lambda e^{-i\Omega T_o} \qquad (11)$$

where $\Lambda = \dfrac{p}{2\left(\omega_1^2 - \Omega^2\right)}$, the baseline solution and the A terms represent the superharmonic or subharmonic perturbations.

Substituting Equation 11 into Equation 10 is an unpleasant task and the full result will not be included here. Suffice to say, the result looks similar to Equation 4. Where that equation included terms with $e^{3i\omega_1 T_o}$, $e^{5i\omega_1 T_o}$, and the like, this result also includes terms such as $e^{i(4\Omega-\omega_1)T_o}$ and $e^{i(3\Omega-2\omega_1)T_o}$.

As with primary resonance, we must solve for an A that eliminates all secular terms. Unlike that problem, however, the presence of Ω in the exponent of e means that we do not have a single equation to solve such Equation 5. Instead, we will have a number of special cases corresponding to any excitation frequency, Ω, that creates a secular term in the equation. For example, terms that include $e^{i(4\Omega-\omega_1)T_o}$ become secular when $\Omega \approx \dfrac{\omega_1}{2}$. Each of these special cases must be solved in turn. With our 11th order polynomial, 22 possible resonances must be considered: $\dfrac{\omega_1}{11}$, $\dfrac{\omega_1}{9}$, $\dfrac{\omega_1}{7}$, $\dfrac{\omega_1}{5}$, $\dfrac{\omega_1}{4}$, $\dfrac{\omega_1}{3}$, $\dfrac{3\omega_1}{7}$, $\dfrac{\omega_1}{2}$, $\dfrac{3\omega_1}{5}$, $\dfrac{2\omega_1}{3}$, $\dfrac{5\omega_1}{7}$, $\dfrac{7\omega_1}{5}$, $\dfrac{3\omega_1}{2}$, $\dfrac{5\omega_1}{3}$, $2\omega_1$, $\dfrac{7\omega_1}{5}$, $3\omega_1$, $4\omega_1$, $5\omega_1$, $7\omega_1$, $9\omega_1$, and $11\omega_1$.

Fortunately, it can be shown that the FRF equation for each of these special cases takes a very standard form, similar to Equation 9:

$$\gamma_1^2 = \mu^2 + (\sigma - \gamma)^2 \tag{12}$$

where σ is the detuning parameter and μ is the damping term. The γ term is calculated just as it was for primary resonance in Equation 7. Because the primary solution for the superharmonics and subharmonics (Equation 11) is more complicated, γ has more terms than before:

$$\begin{aligned}\gamma \equiv \frac{1}{\omega_1}\Bigg[& 3\alpha_3\left(\Lambda^2 + \frac{1}{8}a^2\right) + 5\alpha_5\left(3\Lambda^4 + \frac{3}{2}\Lambda^2 a^2 + \frac{1}{16}a^4\right) + 35\alpha_7\left(2\Lambda^6 + \frac{9}{4}\Lambda^4 a^2 + \frac{3}{8}\Lambda^2 a^4 + \frac{1}{128}a^6\right) \\ & + 63\alpha_9\left(5\Lambda^8 + 10\Lambda^6 a^2 + \frac{15}{4}\Lambda^4 a^4 + \frac{5}{16}\Lambda^2 a^6 + \frac{1}{256}a^8\right) + 231\alpha_{11}\Bigg(6\Lambda^{10} + \frac{75}{4}\Lambda^8 a^2 + \frac{25}{2}\Lambda^6 a^4 \\ & + \frac{75}{32}\Lambda^4 a^6 + \frac{15}{128}\Lambda^2 a^8 + \frac{1}{1024}a^{10}\Bigg)\Bigg]\end{aligned} \tag{13}$$

The parameter γ_1 is calculated for each potential resonance by zeroing the specific terms that would become secular at that frequency. As an example, for $4\omega_1$, γ_1 is defined as follows:

$$\gamma_1 = \frac{a^6\Lambda^2}{\omega_1}\left[\frac{9}{32}\alpha_9 + \frac{165}{16}\alpha_{11}\left(\Lambda^2 + \frac{3}{32}a^2\right)\right]$$

One problem with superharmonics and subharmonics that did not exist in primary resonance is the presence of Λ in the expression for γ_1. Since Λ is a function of σ, this becomes a high-order equation in both a and Λ. At minimum it is 11th order and in many cases it rises to 22nd. It becomes impossible to solve these equations closed-form, so instead they must be solved iteratively. This is a cumbersome process. Developing ways of bounding these solutions to focus the iterations is a future goal of the project.

Fortunately, with a Region I damping of 4.71%, it was possible to show through iteration that the majority of γ_1's calculated did not lead to valid solutions. All special cases created solely through 7th, 9th, or 11th order terms were found to either not have solutions or the solutions were trivially small. Only six cases were found to generate solutions of interest: $\frac{\omega_1}{5}$, $\frac{\omega_1}{3}$, $\frac{\omega_1}{2}$, $2\omega_1$, $3\omega_1$, and $5\omega_1$.

2.3 Ueda Plots

With this data in hand, FRFs can be calculated for any load level. One efficient way to do that is through a diagram similar to the ones developed by Ueda, which are described in Thompson and Stewart [7]. In it, a series of lines trace where the various FRF curves either intersect the knee line or vanish. These lines define regions where various types of the strap dynamic test.

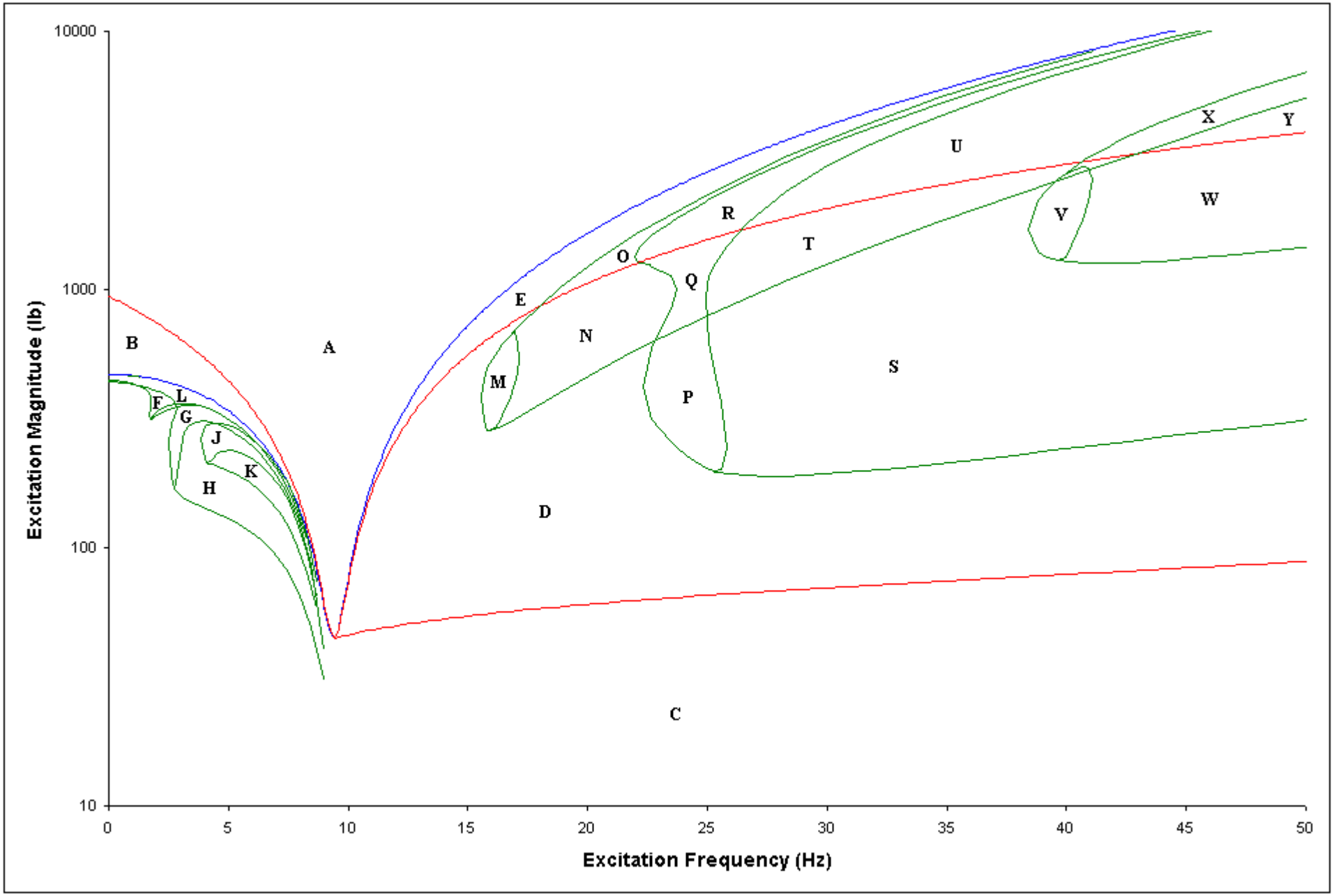

Figure 9: Excitation Magnitude-Frequency Plot For Test Configuration

The lines in Figure 9 come from three primary sources. To aid the explanation, they have been colored to match Figures 6 through 8.

- The blue line traces the movement of the two points where the linear Region I solution intersects with the purple knee line in Figures 6 through 8. Above this line (regions A & B), no linear solution exists. Below that line (regions C, D, and E), a linear solution is possible.

- The red lines track the movement of the nonlinear primary resonant solution. The two lines that follow a similar course to the blue line track the points where the primary resonant solution intersects with the knee line as excitation magnitude increases. The lower, nearly horizontal line tracks the movement of the primary resonant peak. Below these lines (regions B and C), the primary resonant solution does not exist. Above them you have either one valid nonlinear primary resonant solution (regions A and E), or two (region D).

- The green lines show where superharmonic and subharmonic solutions exist. Inside those regions, we would expect to see either one or two valid solutions corresponding to the subharmonic. The specific regions are as follows:
  - Regions F and L – 1 valid $\omega_1/5$ solution
  - Regions G and L – 1 valid $\omega_1/3$ solution
  - Regions H, J, and K – 2 valid $\omega_1/3$ solutions
  - Region J – 1 valid $\omega_1/2$ solution
  - Region K – 2 valid $\omega_1/2$ solutions
  - Region M – 1 valid $2\omega_1$ solution
  - Regions N, O, Q, R, T, U and X – 2 valid $2\omega_1$ solutions
  - Regions P, Q, and R – 1 valid $3\omega_1$ solution
  - Regions S, T, U, V, W, X and Y – 2 valid $3\omega_1$ solutions
  - Region V – 1 valid $5\omega_1$ solution
  - Regions W, X, and Y – 2 valid $5\omega_1$ solutions

Note that for any given region, all these possibilities are cumulative. Table 3 gives a specific breakdown of what steady-state solutions exist by region.

Table 3: Steady-State Solutions by Region

Region	Possible Solutions
A	1 nonlinear primary
B	No steady-state harmonic solutions
C	1 linear
D	1 linear, 2 nonlinear primary
E	1 linear, 1 nonlinear primary
F	1 linear, 1 $\omega_1/5$ superharmonic
G	1 linear, 1 $\omega_1/3$ superharmonic
H	1 linear, 2 $\omega_1/3$ superharmonic
J	1 linear, 1 $\omega_1/2$ superharmonic, 2 $\omega_1/3$ superharmonic
K	1 linear, 2 $\omega_1/2$ superharmonic, 2 $\omega_1/3$ superharmonic
L	1 linear, 1 $\omega_1/3$ superharmonic, 1 $\omega_1/5$ superharmonic
M	1 linear, 2 nonlinear primary, 1 $2\omega_1$ subharmonic
N	1 linear, 2 nonlinear primary, 2 $2\omega_1$ subharmonic
O	1 linear, 1 nonlinear primary, 2 $2\omega_1$ subharmonic
P	1 linear, 2 nonlinear primary, 1 $3\omega_1$ subharmonic
Q	1 linear, 2 nonlinear primary, 2 $2\omega_1$ subharmonic, 1 $3\omega_1$ subharmonic
R	1 linear, 1 nonlinear primary, 2 $2\omega_1$ subharmonic, 1 $3\omega_1$ subharmonic
S	1 linear, 2 nonlinear primary, 2 $3\omega_1$ subharmonic
T	1 linear, 2 nonlinear primary, 2 $2\omega_1$ subharmonic, 2 $3\omega_1$ subharmonic
U	1 linear, 1 nonlinear primary, 2 $2\omega_1$ subharmonic, 2 $3\omega_1$ subharmonic
V	1 linear, 2 nonlinear primary, 2 $3\omega_1$ subharmonic, 1 $5\omega_1$ subharmonic
W	1 linear, 2 nonlinear primary, 2 $3\omega_1$ subharmonic, 2 $5\omega_1$ subharmonic
X	1 linear, 1 nonlinear primary, 2 $2\omega_1$ subharmonic, 2 $3\omega_1$ subharmonic, 2 $5\omega_1$ subharmonic
Y	1 linear, 1 nonlinear primary, 2 $3\omega_1$ subharmonic, 2 $5\omega_1$ subharmonic

It should be noted that four regions were calculated analytically but were not included in Figure 9. They are the $\omega_1/7$, $\omega_1/9$, and $\omega_1/11$ superharmonics and the region where three nonlinear primary resonances are valid. In each case, the region was so small as to be invisible except at the highest resolutions. These regions are too small to be of any practical interest for correlation and will not be considered further. Several other regions were included in the plot but not labeled, because they were quite small and would be of little interest during the testing.

One region of interest during the test will be Region B. That region lies above the blue line in Figure 9, so no linear solutions can exist, but lies below the red line, so no nonlinear solutions can exist. Therefore, according to these equations, no valid steady-state harmonic response exists. It is possible that a chaotic solution would exist in this region. Studying this will be one of the test goals.

3.0 Analytical Comparisons

As previously mentioned, an SDOF Nastran model of the test system was built. This system used the exact nonlinear force-displacement relationship shown in Table 2. As an initial validation of the hand calculations, test cases with different excitation magnitudes and frequencies were run to steady state. The excitation magnitudes ranged from 50 lb to 200 lb in 25 lb increments and the frequencies ranged from 7 Hz to 12 Hz in 1Hz increments. Figure 10 superimposes these cases on the Ueda plot. Both Region I linear and primary nonlinear resonant responses are expected.

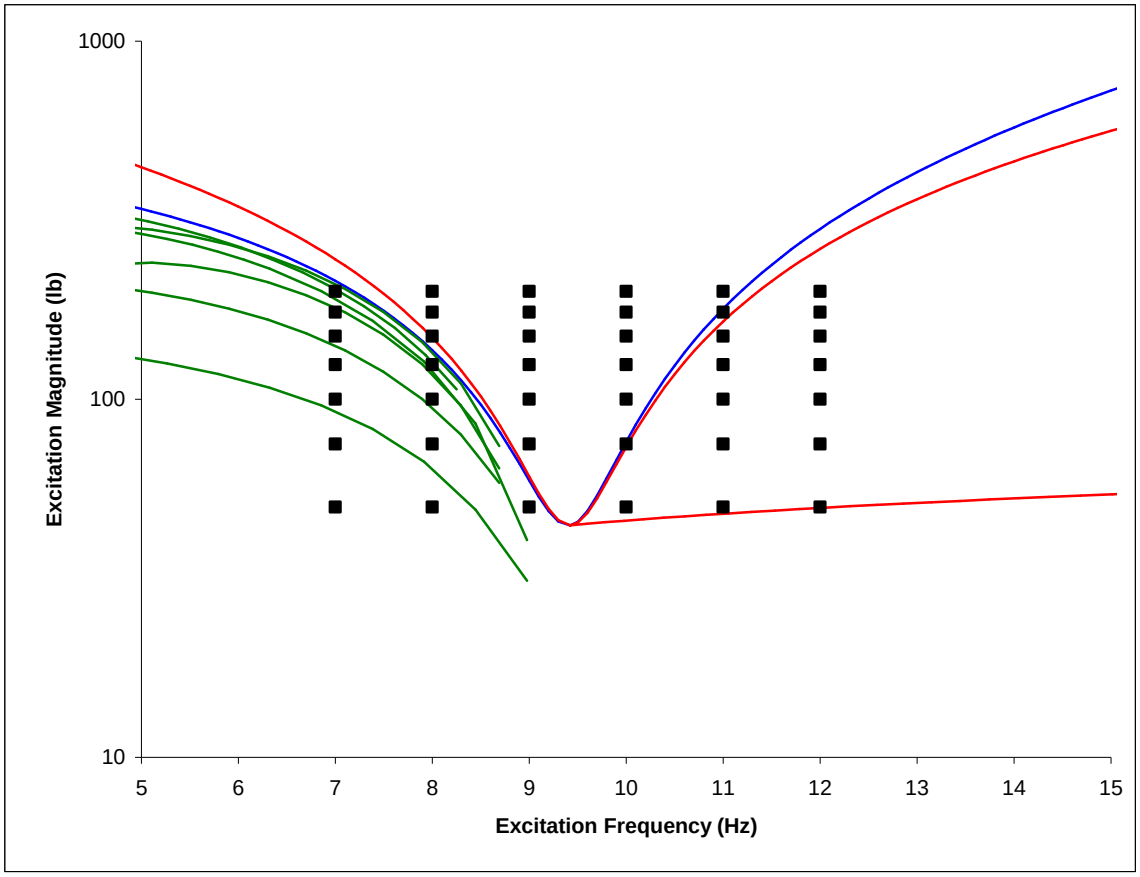

Figure 10: Analytical Comparison Test Cases

Each test case was run for 1000 cycles with a time step equal to 0.1% of the period of the given excitation frequency. After confirming that the system had indeed settled to steady-state, the response magnitude was compared to the iterative predictions using the method described above. The results are shown in Table 4.

Table 4: Predicted Steady-State Magnitudes

	Excitation Frequency					
Excitation Magnitude	7 Hz	8 Hz	9 Hz	10 Hz	11 Hz	12 Hz
200 lb	N: 0.0972” E: 0.0972” D: 0.04%	N: 0.1090” E: 0.1068” D: 2.02%	N: 0.1126” E: 0.1113” D: 1.08%	N: 0.1159” E: 0.1154” D: 0.40%	N: 0.1189” E: 0.1191” D: 0.18%	N: 0.1222” E: 0.1225” D: 0.27%
175 lb	N: 0.0851” E: 0.0851” D: 0.04%	N: 0.1076” E: 0.1055” D: 1.93%	N: 0.1116” E: 0.1103” D: 1.15%	N: 0.1149” E: 0.1145” D: 0.34%	N: 0.1182” E: 0.1183” D: 0.04%	N: 0.0607” E: 0.0609” D: 0.37%
150 lb	N: 0.0729” E: 0.0729” D: 0.04%	N: 0.1057” E: 0.1042” D: 1.46%	N: 0.1105” E: 0.1092” D: 1.20%	N: 0.1140” E: 0.1135” D: 0.47%	N: 0.1174” E: 0.1174” D: 0.00%	N: 0.0520” E: 0.0522” D: 0.37%
125 lb	N: 0.0608” E: 0.0608” D: 0.04%	N: 0.0950” E: 0.0949” D: 0.11%	N: 0.1093” E: 0.1080” D: 1.27%	N: 0.1131” E: 0.1125” D: 0.50%	N: 0.1165” E: 0.1165” D: 0.01%	N: 0.0434” E: 0.0435” D: 0.37%
100 lb	N: 0.0486” E: 0.0486” D: 0.04%	N: 0.0760” E: 0.0759” D: 0.11%	N: 0.1081” E: 0.1066” D: 1.38%	N: 0.1121” E: 0.1114” D: 0.67%	N: 0.0580” E: 0.0581” D: 0.32%	N: 0.0347” E: 0.0348” D: 0.37%
75 lb	N: 0.0365” E: 0.0365” D: 0.04%	N: 0.0570” E: 0.0570” D: 0.11%	N: 0.1063” E: 0.1051” D: 1.12%	N: 0.1110” E: 0.1101” D: 0.79%	N: 0.0435” E: 0.0436” D: 0.32%	N: 0.0260” E: 0.0261” D: 0.37%
50 lb	N: 0.0243” E: 0.0243” D: 0.04%	N: 0.0380” E: 0.0380” D: 0.11%	N: 0.0882” E: 0.0878” D: 0.40%	N: 0.0681” E: 0.0684” D: 0.40%	N: 0.0290” E: 0.0291” D: 0.32%	N: 0.0173” E: 0.0174” D: 0.37%

Note: In each cell, N indicates the NASTRAN prediction while E indicates the iterative prediction (from Microsoft Excel). The bold line delineates the two different solution types: below the line NASTRAN converged to the Region I linear solution, while above the line NASTRAN converged to the primary resonant nonlinear solution. D indicates the percent difference between the two.

A quick look at the comparison shows that both the Region I linear and primary nonlinear resonant solutions match up well. All solutions were of a type that was predicted to be possible at that combination of excitation frequency and magnitude. This gives us some confidence that the regions outlined in Figure 9 are correct.

4.0 Test Cases

As previously mentioned, the primary goal of this test is to verify the accuracy of Figure 9. Based on this analysis, the following test cases are proposed (shown graphically in Figure 11):

1) **A smart hammer test**. The goal of this would be to observe the system decay and calculate the damping value.
2) **A sine sweep from 5-50 Hz with 40 lbs excitation force, sweeping up and down.** This is a standard sine sweep test to confirm the strap Region I dynamic properties.
3) **A sine sweep from 5-100 Hz with 100 lbs excitation force, sweeping up and down**. This case studies the nature of the knee point, where both the linear and nonlinear solutions meet. It should be possible to capture the entire primary resonant peak.
4) **A sine sweep from 5-100 Hz with 250 lbs excitation force, sweeping up and down.** This case will study another set of data points for the linear-nonlinear junction as well as passing through two of the subharmonic solution regions.
5) **A sine dwell at 6 Hz with 300 lbs excitation force.** This will put the system squarely in Region B and allow collection of data for that unusual region.
6) **A sine dwell at 12 Hz with the excitation force slowly increasing from 30 lbs to 300 lbs, sweeping up and down.** This would be a third set of data points for the linear-nonlinear junction, obtained from a different perspective.
7) **Sine dwells at 25 Hz with different force levels that change during the dwell to 250 lbs.** 250 lbs at 25 Hz puts the system in region P. Starting the system at various force levels and allowing it to come to a steady-state solution allows us to vary the initial conditions for our SDOF system. The goal is to get the system to reach different steady-state solutions with the same forcing function. Region K has four separate solutions to work with.

The primary correlation targets are regions A, B, C, D, and E. The superharmonic and subharmonic solutions are of interest, but achieving a steady-state response of that type based on a simple sweep is expected to be difficult. Initial nonlinear transient runs indicate that when starting from rest, the system prefers to come to the linear steady-state solution, if available, and the primary nonlinear resonant solution if it is not. It is therefore not expected that we will see any superharmonic or subharmonic behavior except in the final 250 lb/25 Hz test case, where we are specifically seeking it. Confirmation of the “priority” of the various solutions will be another goal of this test.

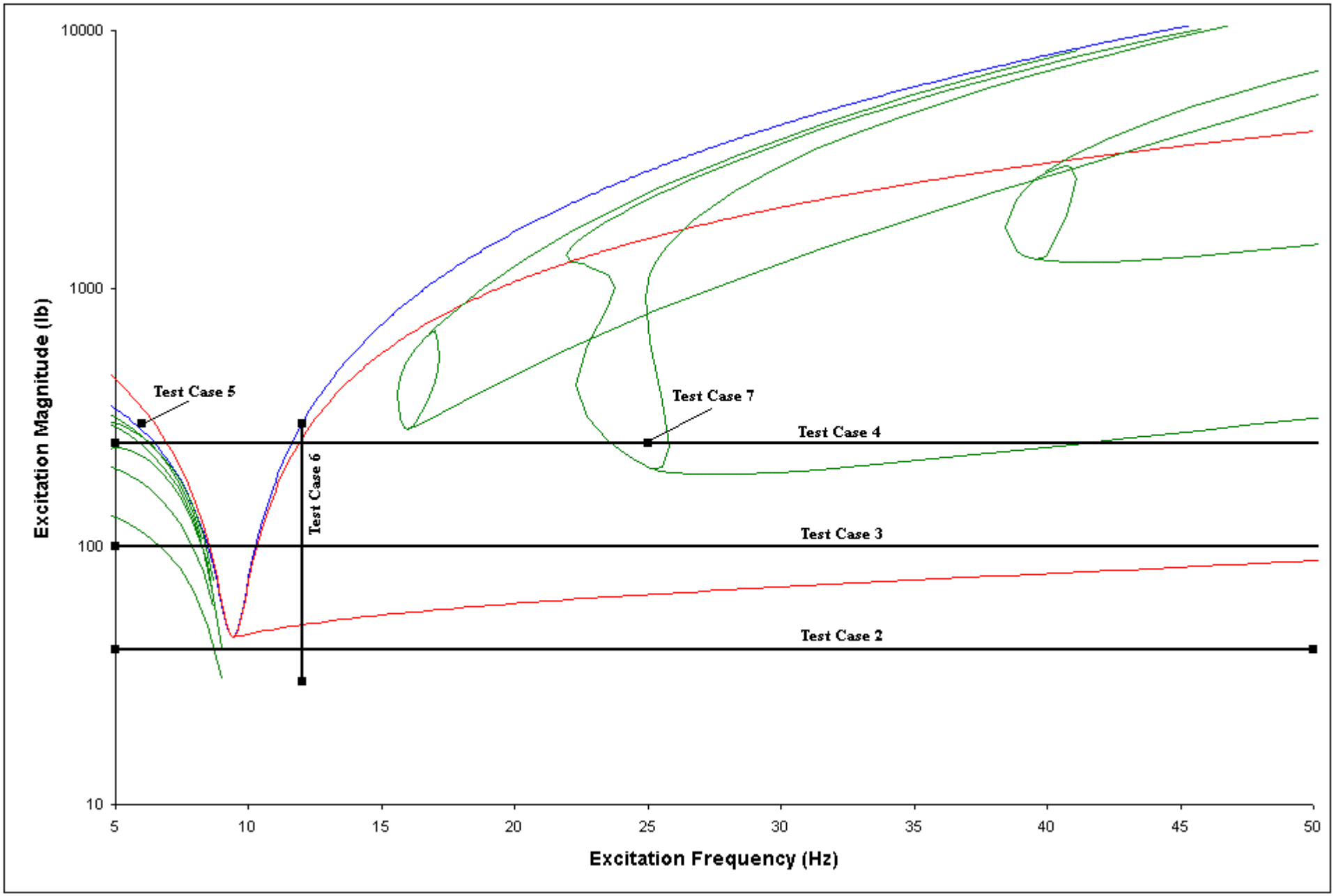

Figure 11: Test Cases for Strap Dynamic Test